Available online at www.sciencedirect.com
SciVerse ScienceDirect
ELSEVIER
Procedia Engineering 26 (2011) 1756 – 1764
Procedia Engineering
www.elsevier.com/locate/procedia

First International Symposium on Mine Safety Science and Engineering

# Identification methods of the deformation memory effect in the stress region above crack initiation threshold

Haijun Wang[a]*, Xuhua Ren[a], Ranran Tao[a]

[a]Hohai University, NO.1 Xikang Rd, Nanjing 210098, China

**Abstract**

Deformation memory effect (DME) is one of the rock memory effects. One important application of the DME is to determine the *in situ* stress state. Compared to the traditional *in situ* stress measurements, the methods based on the DME are commercial and permit large number of measurements. Application of DME needs enough reliable identification methods. However, the existing methods sometimes are indistinct and the amount is insufficient. combined with three traditional methods including tangential modulus method, deformation rate analysis (DRA), acoustic emission method, two new potential methods were explored in the stress region above crack initiation threshold. One is based on the fractal dimension, called FD method. Another one is to take advantage of the lateral strain in the DRA method and the FD method, instead of using the axial strain. Based on the contact bond model in PFC$^{2D}$, numerical model for granite sample was developed and cyclic uniaxial compressions were performed on it. Both the existing methods and new methods were used to detect the DME. The results demonstrate that the FD method is effective and reliable, result by DRA method with lateral strain is better than that with the axial strain, the tangential modulus method is not so distinct as other methods.


Selection and/or peer-review under responsibility of China Academy of Safety Science and Technology, China University of Mining and Technology(Beijing), McGill University and University of Wollongong.

*Keywords:* Deformation memory effect; Identification methods; *In situ* stress; PFC$^{2D}$

## 1. Introduction

Memory effect is a natural ability of the brittle and ductile rocks to keep the information about experienced actions [1]. It includes many memory effects, such as deformation memory effect (DME), acoustic emission memory effect (AEME), also called Kaiser effect [2], electric memory effect [3],

* Corresponding author. Tel.: +61-0432087624.
*E-mail address*: haijun@civil.uwa.edu.au.

1877-7058 © 2011 Published by Elsevier Ltd. Open access under CC BY-NC-ND license.
doi:10.1016/j.proeng.2011.11.2364

thermal emission memory effect in cyclic heating [1] and so on. The DME takes place in the rock samples subjected to cyclic loadings. When the peak stress previously applied is attained in the following loading, a change in the stress-strain curve occurs, called as DME. In the stress region above the crack initiation threshold, crack propagation and generation can be expected. In this region, cracks contribute to the change of the stress-strain curve as one of sources of inelastic strain. Therefore, along with DME, acoustic emission activities increase dramatically when the previous maximum stress is attained in this region, known as Kaiser effect (KE or AEME).

One of the important applications of AEME and DME is to determine the *in situ* stress state [4,5], which is essential for not only understanding basic geological process but also the design work for underground projects in and on rock masses [6]. Compared to the traditional *in situ* stress measurement such as hydraulic fracturing method and overcoring method, the methods based on the DME are done in the laboratory by special loadings on samples extracted from cores, thus commercial and permit large numbers of measurements. Another advantage is that the methods based on the DME are not influenced by the anisotropic elastic modulus of the rock.

The application of the DME needs a number of reliable and effective identification methods. Logically, if one method does not work well, other methods will be needed to provide additional information to detect the DME. However, until now, only the deformation rate analysis (DRA) method with the axial strain was developed and commonly used [5, 7-9]. What is worse, in many cases, the DRA method is indistinct and subjective by naked eyes. This problem can be seen in many previous studies [7-9]. Therefore, it is important to develop more identification methods for the DME.

In this paper, in addition to the DRA method using axial strain, the following methods were introduced, direct identification method using tangential modulus, DRA method using lateral strain, fractal dimension (FD) method and acoustic emission (AE) method. Firstly, the detailed descriptions for these methods were given in section 2. Secondly, the numerical model for granite sample based on the contact-bond model in the two dimension particle flow code ($PFC^{2D}$) was developed. Uniaxial compression tests were performed on the model in the stress region above the crack initiation threshold. All the methods introduced were used to detect the DME. The results demonstrate that, except the direct identification method, DRA method using lateral strain, the FD method using both axial and lateral strain and AE method can supply an accurate and effective identification of the DME.

## 2. Deformation Memory Effect Identification Methods

### *2.1. Direct identification method using modulus*

In this method, two cycles of uniaxial compressive loading are performed on the rock specimens excavated from rock cores. According to the definition of the DME, there is a change in the stress train curve when the previous maximum stress is attained. Therefore, the direct identification method is to track the change of the local tangential modulus of the stress-train curve in the first loading [10]. The stress value at the decrease point in the stress-tangential modulus curve is regarded as the normal stress component of previous maximum stress or *in situ* stress. In order to further tell clearly the location of the changing point, the tangential modulus in the second loading should also be given as a comparison [11]. In this paper, moving point regression technique was used in the computation of the local tangential modulus [12].

### *2.2. Deformation rate analysis (DRA method)*

The deformation rate analysis (DRA) was proposed in 1990 [5]. In the DRA method, the strain difference function $\Delta\varepsilon_{i,j}(\sigma)$ was introduced and defined for a pair of the $i^{th}$ and the $j^{th}$ loading cycle on rock samples by

$$\Delta\varepsilon_{i,j}(\sigma)= \varepsilon_j(\sigma)- \varepsilon_i(\sigma) \qquad (1)$$

Here, $\varepsilon_i(\sigma)$ denotes the axial strain in the $i^{th}$ loading stage, σ is the applied axial stress correspondingly. The strain difference function is illustrated in Fig. 1.

By this function, the normal component of the previous peak stress or *in situ* stress in the direction of the compression on the rock can be determined at the inflection point of the curve of $\Delta\varepsilon_{i,j}(\sigma)$ (DRA curve). Generally, the inflection of the $\Delta\varepsilon_{i,j}(\sigma)$ curve was recognized by naked eyes and thus subjective. This method can only work when the bending is unique and very obvious.

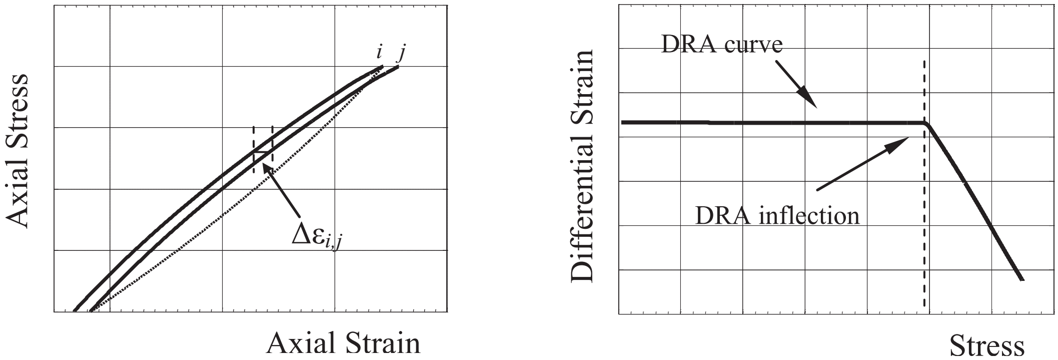


Fig. 1. Illustration of the DRA method. (a) is the definition of the function $\Delta\varepsilon_{i,j}(\sigma)$. (b) shows the curve of $\Delta\varepsilon_{i,j}(\sigma)$ (DRA curve) and the definition of the DRA inflection (After Yamamoto [8])

In most previous studies, only the axial strain – stress data was used in the DRA method. However, in the stress region above crack initiation threshold, the lateral strain is more sensitive to the cracks parallel to the axial stress than the axial strain [13]. In this paper, not only the axial stress-strain data points were analyzed, but also the axial stress-lateral strain was analyzed using the DRA method.

### *2.3. Fractal dimension method (FD method)*

The concept and mathematical properties of the fractal were established by Mandelbrot [14]. For a regular smooth curve, its fractal dimension is 1, while greater than 1 for a fractal curve. Based on the fractal dimension theory, the value of D is directly proportional to the irregularity of the curve. Therefore, if we divide a curve into small segments, the change of irregularity in the whole curve can be attained by the change in fractal dimension of the small segments. This method is called as FD method and used to reveal the irregularity change of a fractal curve. The FD method has been successfully applied in many fields, such as analysis of lung and bowel sound signals [15] and damage detection in the structure [16].

As to the mechanism of the DME, it may be frictional sliding over the crack interfaces and/or cracks, and/or other inelastic sources for different rocks in different deformation stages. However, no matter what it is, the change of the internal behavior in rock would shift the irregularity of the stress-strain curve. Consequently, by means of FD method, the irregularity variations are linked with the changes of the stress-strain curve of the second loading before and after the memory effect point, providing a fast computational tool that tracks the deformation memory. It should be noted that, the FD method is not used to identify fractal characteristics of the inelastic source or stress-strain curve, but to identify the variations in their irregularity. Therefore, the normal component stress of previous maximum stress or *in situ* stress is accurately captured at the abruptly increase of the FD value.

To divide the stress-strain curve into small segments, a window with a fixed size sliding along with the curve is used, and the FD is then calculated for every small segment falling into the sliding window, shown in Fig. 2. According to Katz's theory [17], the FD of a small segment in a stress-strain curve is defined by:

$$FDM(x)=\log(n)/(\log(n)+\log(d(x_i,M)/L(x_i,M))) \quad (2)$$

$$L(x_i,M)=\sum((y(x_{i+j})-y(x_{i+j-1}))^2+(x_{i+j}-x_{i+j-1})^2)^{0.5}, \quad (j=1\ldots M) \quad (3)$$

$$d(x_i,M)=\max_{1\le j\le M}((y(x_{i+j})-y(x_i))^2+(x_{i+j}-x_i)^2)^{0.5} \quad (4)$$

Where, the term M represents the number of points falling in the sliding window. $x=0.5(x_i+x_{i+M})$, $n=L/a$, the term "a" is the average of distance between successive points. L is the length of the curve. It should be noted that, $y=\sigma/10^{10}$, $x=\varepsilon$ in the FD computation for stress-strain curve in this paper.

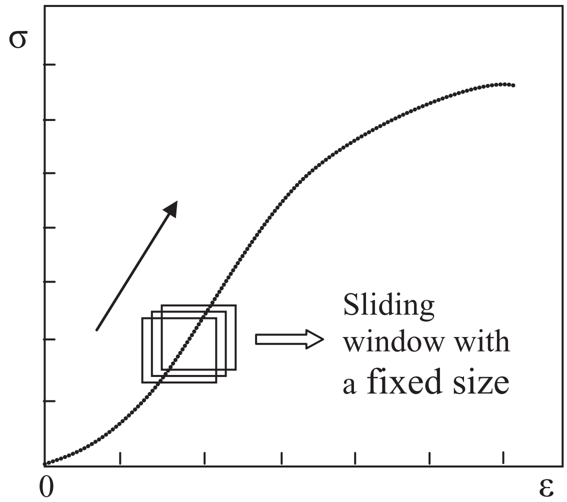


Fig. 2. The sliding window with a fixed size.

At each window, the FD value is calculated using equation (2), and the value is assigned to the midpoint of the sliding window. In this way, point-to-point values of the estimated FD were obtained.

Same as that in other fields with FD method, the FD value computed at each point depends on the size of the sliding window. Small-scale fluctuations in FD curve would be filtered out when the window size is extremely large. However, it was found that the general shape of the FD curve remained the same with increasing sliding window size. As treated by other researchers using FD method, in problems where the identification of rock deformation memory effect is the primary aim. In this case, it appears that, the true value of the FD is not as important as the changes in FD curve associated with the DME. In our numerical experiments, 10 stress strain data points were used as the window size.

## *2.4. Acoustic emission method*

As mentioned in previous section, in the stress region above crack initiation threshold, Kaiser effect takes place in rocks and materials subjected to loading cycles. It is widely accepted that, the cracks contribute to the irreversible inelastic deformation. Thus in this stress region, the Kaiser effect occurs along with the DME. Therefore, the acoustic emission (AE) events can also used as an identification method for the DME, called AE method. There are two methods to process the AE events [4], "cumulative AE hits versus stress" and "AE hit rate versus stress". The DME or KE can be recognized at the abruptly increase point in the curve of "cumulative AE hits versus stress" and curve of "AE hit rate versus stress". In this paper, the former one is used.

However, it should be noted that, no proves indicated that, the crack propagation and generation is the only source that accounts for the DME.

## 3. Application of the Methods in Numerical Experiments

In order to better understand the DME and its identification methods, the numerical analysis was conducted in this paper. The characteristic resulting from numerical analysis can also be used to guide the physical experimental study. In this paper, a numerical model for granite was developed based on the contact-bond model in $PFC^{2D}$. $PFC^{2D}$ allows the user to explicitly model fracture damage directly using a discrete-element modeling algorithm and thus has an advantage over a continuum modeling approach.

As for the contact-bond model in the $PFC^{2D}$, the interaction between two particles is determined by the contact bond with constant normal and shear stiffness acting at the contact point. The shear and tensile strength values are assigned to the contact bond. If the normal contact bond strength or the shear contact bond strength is exceeded, the bond breaks, which is considered to be analogous to the formation of a micro-crack, which presents an acoustic emission event. The frictional sliding will occur when the shear strength was exceeded. As a result, the internal micro-mechanical behavior in the rock can be simulated.

### *3.1. Numerical model and the methodology*

A numerical model for Aue granite was simulated based on the contact bond model. The micro-parameters has already been verified reliable by Yoon [18], listed in the Table 1. The size of the round particles is ranging from 0.25mm to 0.415mm. The shape of the numerical model is rectangle, shown in Fig. 3, and its physical properties are listed in Table. 2.

Table 1. Micro-parameters of the numerical model for the granite

| $PFC^{2D}$ micro-parameter | | Unit | Value |
|---|---|---|---|
| Ball contact modulus | $E_c$ | GPa | 96.6 |
| Ball stiffness ratio (normal stiffness over shear stiffness) | kn/ks | – | 2.5 |
| Ball friction coefficient | $\mu$ | – | 0.44 |
| Mean contact-bond normal strength | $\sigma_c$ (mean) | MPa | 100.0 |
| Std. deviation of the mean contact-bond normal strength | $\sigma_c$ (S.D.) | MPa | 32.0 |
| Mean contact-bond shear strength | $\tau_c$ (mean) | MPa | 200.0 |
| Std. deviation of the mean contact-bond shear strength | $\tau_c$ (S.D.) | MPa | 64.0 |

Table 2. Macro-properties of the numerical model

| Model | Dimensions w×h(mm) | UCS (MPa) | Young's modulus (GPa) | Poisson's ratio (-) | Crack initiation (MPa) |
|---|---|---|---|---|---|
| Granite | 55×110 | 142.4 | 67.0 | 0.24 | 24.6 |

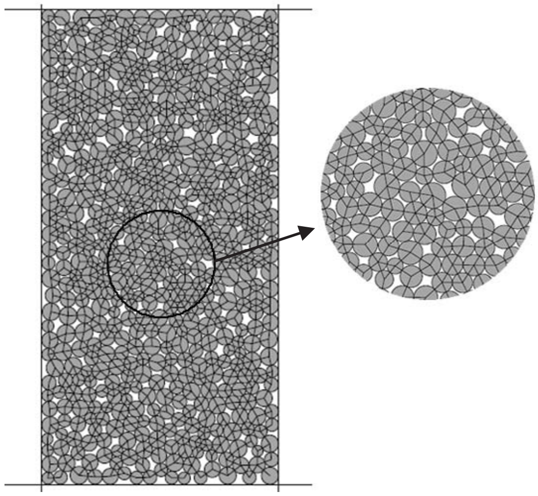

Fig. 3. The numerical model for granite. Black lines are contact bonds connecting the particles.

Three axial compression loading cycles were performed on the numerical model. The loading and unloading were controlled by platens velocity, which was 0.05m/s. The first loading cycle was used to initiate the deformation memory information of the peak stress value “$\sigma_p$”. The second and third loadings were used as measuring loading cycles with the same peak stress value “$\sigma_m$”, which was greater than “$\sigma_p$”. The first measuring loading cycle was used in FD method and AE method. Two measuring loading cycles were used in the DRA method. The loading regime was 60-80-80MPa, shown in the Fig. 4 (a). The stress-strain curve is shown in the Fig. 4 (b). It should be noted that, all the peak stress value in the three loading cycles were great higher than the crack initiation threshold. In other words, the loading regime was performed in the region where cracks were expected.

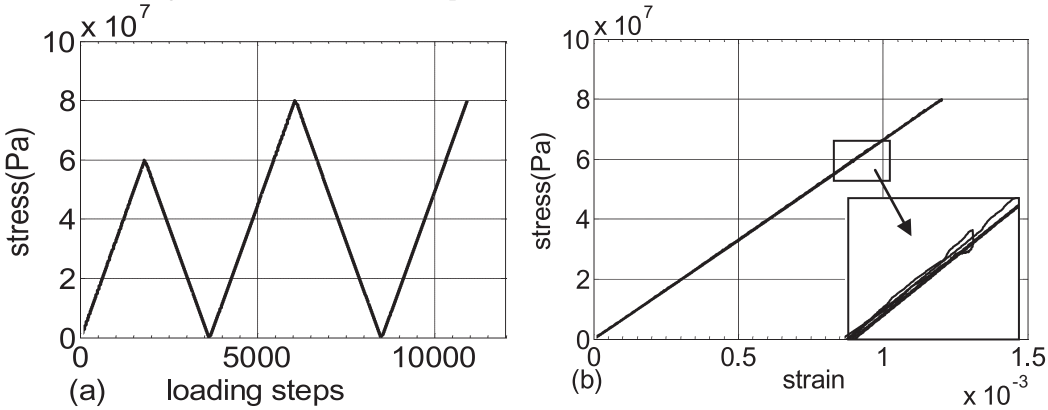


Fig. 4. (a) is the loading regime. (b) is the stress-strain curve.

### 3.2. Result of the direct method using tangential modulus

The local tangential modulus was computed in the second and the third loading. The result is shown in Fig. 5. As mentioned above, there should be a sharp decrease in the curve of tangential modulus versus stress at previous maximum stress $\sigma_p$. From Fig. 5 (a) it can be seen that, the average of the tangential modulus value in the range from about 58MPa to 80MPa was slightly lower than that in the former stress region. This phenomenon is in accordance with the description of the tangential modulus method. However, in the range from 58MPa to 80MPa, the modulus changed with violent fluctuations which made accurate identification for the DME very difficult. In consideration of the influences of other factors in the physical experiments, the detection of the DME will become more indistinct and subjective by this method. Therefore, we do not recommend this method in identification of the DME.

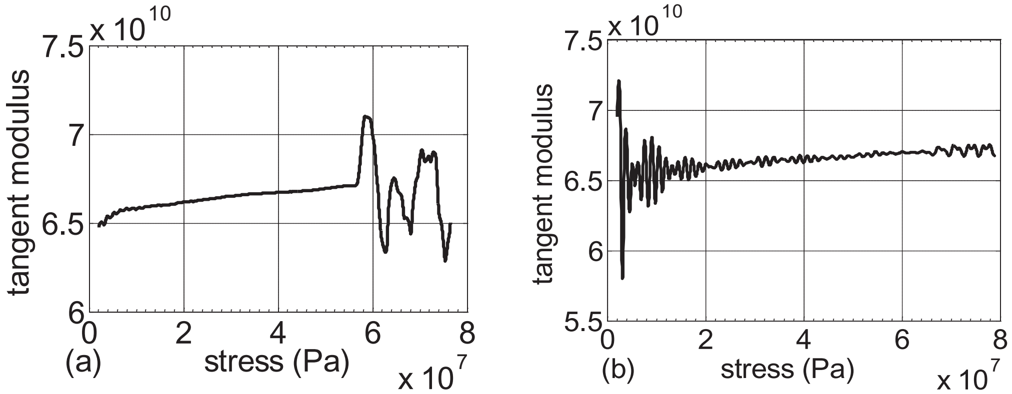


Fig. 5. The local tangential modulus vs. stress. (a) is that in the second loading. (b) is that in the third loading.

### *3.3. Result of the DRA method*

In the numerical analysis, the differential strain was computed using equation (1), here, $\Delta\varepsilon_{2,3}(\sigma)=\varepsilon_3(\sigma)-\varepsilon_2(\sigma)$. Traditionally, the axial strain and axial stress data was used in the equation (1) in the DRA method. In this paper, not only the axial stress - axial strain but also the axial stress - lateral strain were used. The result is shown in Fig. 6. It can be seen from Fig. 6, there was an inflection point in both the differential axial strain curve and differential lateral strain curve at $\sigma_p$. As mentioned in previous section, the lateral strain is more sensitive to the cracks parallel to the axial stress than the axial strain. It is verified from the comparison of Fig. 6 (a) and (b). In the differential lateral strain curve, the downtrend was more obvious than that in the differential axial strain curve. It indicated that, in the stress region above the crack initiation stress, the DRA method with the differential lateral strain is more distinct and reliable than that with differential axial strain.

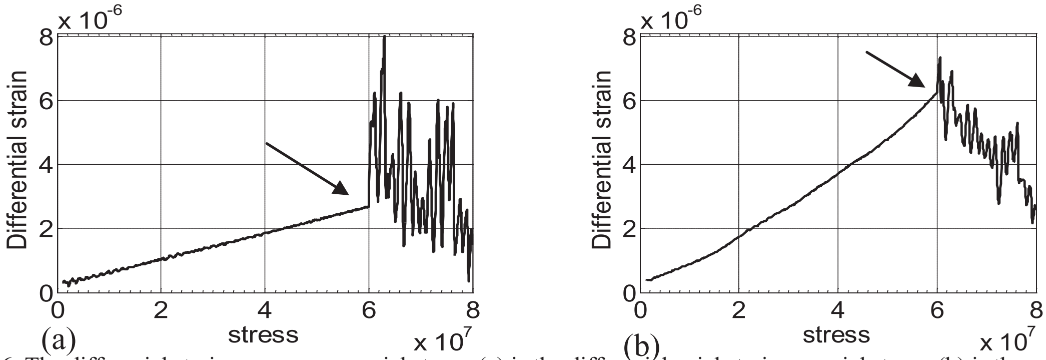


Fig. 6. The differenial strain curve versus axial stress. (a) is the differenial axial strain vs. axial stress. (b) is the differenial lateral strain vs. axial stress.

### *3.4. Result of the FD method*

The FD method was employed on both axial stress - axial strain data and axial stress - lateral strain data in the second loading in the numerical tests. Fig. 7 displays the FD curve in the second loading. It is obvious that the FD value increases sharply after the previous peak stress $\sigma_p$. It is verified that the FD method with both lateral strain and axial strain can be an accurate DME identification method.

Further, from Fig. 7, abruptly increase of the FD value reveals that, the irregularity of the stress strain curve increases when $\sigma_p$ is exceeded, which is in accordance with the description in the previous section. In other words, the previous loading makes the stress-strain curve more smooth in the same stress region in the following loading.

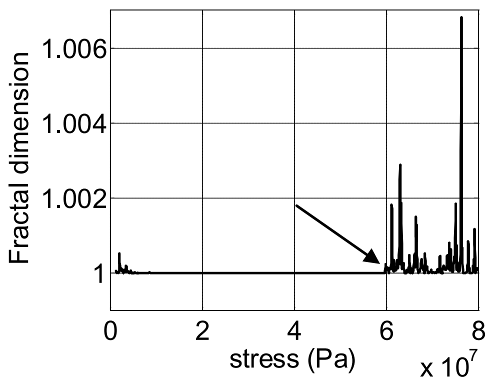


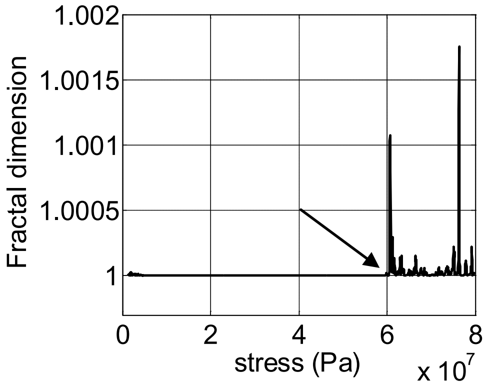


Fig. 7. The FD curve versus axial stress in the second loading. (a) takes advantage of axial strain. (b) takes advantage of lateral strain.

### 3.5. Result of the AE method

In the second loading, the cumulative cracks number was recorded. Every crack event is analogical to one acoustic emission event in the PFC$^{2D}$, thus the cumulative cracks number can be also considered as cumulative AE hits number. The result by the AE method is shown in Fig. 8. It can be seen that, the cumulative cracks number increased sharply at the previous maximum stress value $\sigma_p$.

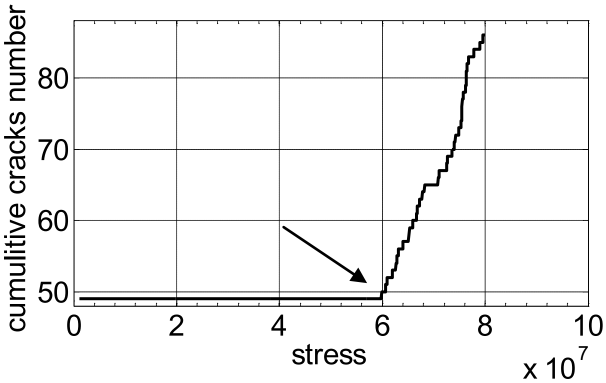


Fig. 8. The cumulative cracks number versus stress in the second loading.

## 4. Conclusions

Methods based on the DME have been used to determine the *in situ* stress for a long time. However, the existing identification methods of DME are limit and sometimes indistinct. Four methods are introduced and discussed in the numerical experiments based on the contact model in PFC2D.

From the results, the direct method using tangential modulus is not reliable, thus it is not recommended. The DRA curve using lateral strain is more distinct than DRA curve using axial strain data. The FD method using the lateral strain or the axial strain is reliable. In the stress region above crack initiation threshold, the Kaiser effect occurs along with the DME, therefore, the AE method can also be a additional method to identification the DME. The FD method and AE method are simpler than DRA method, because of only one loading is needed in the identification of DME for the former two methods.

## Acknowledgements

This work was financially supported by and the Fundamental Research Funds for the Central Universities in China (2010B13914) and Jiangsu 2010 College Graduate Student Research and Innovation Program Foundation (CX10B_215Z).

## References

[1] Yamshchikov VS, Shkuratnik VL, Lavrov AV.Memory effects in rocks. Journal of Mining Science 1994; 30:463-73.

[2] Kaiser J. Information and conclusions from the measurement of noises in tensile stressing of metallic materials. Arch Eisenhuttenwesen 1953; 24: 43–5.

[3] Fujii N, Hamano Y. Anisotropic changes in resistivity and velocity during rock deformation. In High pressure research: application in geophysics. New York: Academic Press; 1997.

[4] Lavrov A. The Kaiser effect in rocks: principles and stress estimation techniques. Int J Rock Mech Min Sci 2003; 40:151–71.

[5] Yamamoto K, kuwahara Y,Kato N, Hirasawa T. Deformation rate analysis: A new method for *in situ* stress estimation from inelastic deformation of rock samples under uni-axial compressions, Tohoku Geophys. Journ.(Sci. Rep. Tohoku Univ., Ser. 5) 1990; 33:127-47.

[6] Fairhurst C. Stress estimation in rock: a brief history and review. Int J Rock Mech Min Sci 2003; 40:957- 73.

[7] Utagawa M,Seto M, Katsuyama K. Estimation of initial stress by deformation rate analysis (DRA). Int J Rock Mech Min Sci 1997; 34: 317.e1-317.e13.

[8] Yamamoto K,Yabe Y. Stress at sites close to the Nojima Fault measured from core samples. The Island Arc 2001;10:266-81.

[9] Villaescusa E, Seto M, Baird G. Stress measurements from oriented core. Int J Rock Mech Min Sci 2002; 39: 603-15.

[10] Horibe T, Kobayashi R. Physical properties of coal-measures rocks under tri-axial pressure. J. Min. Soc 1958;74:142-46.

[11] Makasi M, Fujii Y. Effects of strain and temperature on tangent modulus method. Poceedings of Korean rock mechanics symposium. 2008:279-85.

[12] Eberhardt E, Stead D, Stimpson B, Read RS. Identifying crack initiation and propagation thresholds in brittle rock. Can. Geotech. J 1998; 35: 222-33.

[13] Lavrov A. Fracture-induced physical phenomena and memory effects in rocks: a review. Strain 2005; 41: 135-49.

[14] Mandelbrot B.How long is the coast of Britain? Statistical self-similarity and fractional simension.Science 1967;156:636-8.

[15] Hadjileontiadis LJ, Rekanos IT. Detection of explosive lung and bowel sounds by means of fractal dimension. IEEE Signal Processing Letters 2003;10: 311–14.

[16] Qiao PZ, Lestari W, Shah MC, Wang J. Dynamics-based damage detection of composite laminated beams using contact and noncontact measurement systems. J Compos Mater 2007; 41:1217-52.

[17] Katz MJ. Fractal and the analysis of waveforms. Computers in Biology and Medicine 1988; 18:145-56.

[18] Yoon J. Application of experimental design and optimization to PFC model calibration in uniaxial compression simulation. Int J Rock Mech Min Sci 2007; 44: 871-89.